Submit to Journal of Materials Research and Technology (2017)

Examining the microhardness evolution and thermal stability of an Al-Mg-Sc alloy processed by high-pressure torsion at a high temperature

Pedro Henrique R. Pereira[a,b,*], Yi Huang[a] and Terence G. Langdon[a]

[a]Materials Research Group, Faculty of Engineering and the Environment
University of Southampton, Southampton SO17 1BJ, U.K.

[b]CAPES Foundation, Ministry of Education of Brazil, Brasília - DF 70040-020, Brazil.

Abstract

An Al-3%Mg-0.2%Sc alloy was solution treated and processed through 10 turns of high-pressure torsion (HPT) at 450 K. Afterwards, the HPT-processed alloy was annealed for 1 hour at temperatures ranging from 423 to 773 K and its mechanical properties and microstructural evolution were examined using microhardness measurements and electron backscattered diffraction (EBSD) analysis. The results demonstrate that HPT processing at an elevated temperature leads to a more uniform microhardness distribution and to an early saturation in the hardness values in the Al alloy compared with high-pressure torsion at room temperature. In addition, detailed EBSD analysis conducted on the HPT-processed samples immediately after annealing revealed that the Al-Mg-Sc alloy subjected to HPT processing at 450 K exhibits superior thermal stability by comparison with the same material subjected to HPT at 300 K.

Keywords: Aluminium alloys, Hall-Petch relationship, Hardness, High-pressure torsion, Severe plastic deformation, Thermal stability.

*Corresponding author: Pedro Henrique R. Pereira (email: phrp1d13@soton.ac.uk)

1. Introduction

There is an increasing interest in the development of Al alloys with improved mechanical properties in order to substitute heavier materials in vehicle components and reduce the energy consumption in the transportation industry [1]. Severe plastic deformation (SPD) procedures [2,3] are now recognized as effective methods in fabricating Al alloys with exceptionally small grain sizes within the submicrometre range [4]. Although various SPD techniques are now available, major focus has been dedicated to equal-channel angular pressing (ECAP) [5] and high-pressure torsion (HPT) [6] as these procedures require simple facilities and permit the processing of difficult-to-work materials by controlling the temperature, the imposed pressure and the effective strain rate in the work-pieces [7].

Ultrafine-grained (UFG) Al-Mg alloys exhibit improved mechanical strength by comparison with the material subjected to conventional metal forming [8-12]. The addition of magnesium in this material delays its recovery kinetics and promotes further grain refinement during processing by ECAP [8-10] and HPT [11,12]. Nevertheless, UFG Al-Mg alloys display significant grain coarsening after annealing at relatively low temperatures [13,14] and scandium is added to this material in order to enhance its microstructural stability and thereby preserve the benefits achieved during severe plastic deformation [15-18].

Excellent thermal stability and superplastic properties are documented for Al-Mg-Sc alloys processed by ECAP [19-21]. The Al-3Mg-0.2Sc alloy processed by ECAP at room temperature has an average grain size of ~0.2 μm immediately after processing and achieves a maximum elongation of ~2580 % during tensile testing at 723 K at 3.3×10^{-3} s^{-1} [19]. By contrast, the Al-5Mg-0.2Sc-0.08Zr alloy has a grain size of ~1 μm after ECAP processing at 598 K, however this alloy exhibits superior superplastic properties with a record elongation of ~4100 % attained at 5.6×10^{-2} s^{-1} at 723 K [21]. This outstanding superplastic behaviour is attributed to a larger proportion of high-angle grain boundaries and to an improved microstructural stability in the material processed by ECAP at 598 K.

Recent investigations have demonstrated that HPT processing at elevated temperatures leads to slightly larger grain sizes and lower hardness values in Mg alloys [22,23], stainless steel [24,25] and pure Ni [26] by comparison with HPT at ambient temperature. Conversely, these materials usually have more stable grain structures when annealed after HPT [24-26] and display higher superplastic elongations, as reported for the AZ61 [22] and the Mg-9Al alloy [23]. Accordingly, processing by HPT at high temperatures has emerged as a promising strategy to delay the grain coarsening kinetics in Al-Mg-Sc alloys and retain submicrometre grains at temperatures suitable for superplastic forming.

Therefore, the present study was initiated to evaluate the thermal stability of an Al-3Mg-0.2Sc alloy subjected to 10 turns of HPT processing at 450 K by examining the mechanical properties and microstructural evolution in this UFG material after systematic annealing for 1 h at temperatures ranging from 423 to 773 K.

2. Experimental material and procedures

The material used in this study was an Al-3% Mg-0.2% Sc (in wt. %) alloy supplied by China Rare Metal Material Corporation (Jiangxi Province, China) as forged bars with ~130 mm length and 10 mm diameter. These bars were solution treated at 880 ± 2 K for 1 h and quenched in water. Afterwards, discs with a thickness of ~1 mm were cut from the solution treated material and then ground to a final thickness of ~0.8 mm.

The discs were processed by HPT processing under quasi-constrained conditions [27,28] at 450 ± 5 K. The elevated processing temperatures were achieved by incorporating small heating elements around the upper and lower anvils and the temperature was controlled by a thermocouple placed within the upper anvil at a position of ~10 mm from the HPT sample as described in earlier investigations [22,23,29]. Initially, in the compression stage of HPT processing [30], the discs were compressed within the shallow central depression of the anvils already heated at ~450 K under a nominal pressure of 6.0 GPa. Thereafter, the facility was held

at the processing temperature for ~10 min and finally the lower anvil was rotated at a constant rate of 1 rpm for 10 turns imposing high torsional straining within the HPT sample.

Following HPT processing, discs were annealed at temperatures from 423 to 773 K for 1 h and cooled in air. Afterwards, both the HPT-processed material and the annealed samples were ground and polished to obtain mirror-like surfaces and hardness measurements were then taken at the middle-section of the samples using the same procedure as in other studies [31-33]. Hardness values were evaluated along the diameters of the discs at positions separated by 0.3 mm such that the microhardness in each position was calculated as the average of the measurements taken from four indentations separated by 0.15 mm. Furthermore, the area-weighted average microhardness of the Al-3Mg-0.2Sc alloy was estimated using the hardness measurements recorded along the diameters of the discs and noting that the hardness values near the edges of the sample are associated with larger surface areas. The microhardness values were recorded using an FM300 microhardness tester equipped with a Vickers indenter under a load of 200 gf and a dwell time of 15 s.

The grain structures of the UFG metal was analysed by scanning electron microscopy (SEM) and electron backscattered diffraction (EBSD). Discs were ground, polished using 1 μm diamond paste and 0.06 μm colloidal silica and thereafter etched using a solution of 5 % HBF_4 dissolved in water. The microstructure of the Al alloy was examined using a JSM6500F thermal field emission scanning electron microscope and the average grain size, *d*, was estimated using the linear intercept method. EBSD patterns were collected for the materials annealed at 573, 623 and 773 K using step sizes as small as 0.06 μm. A cleaning procedure, including grain dilatation, was performed after data collection such that the total number of modified points was <20 %. High-angle grain boundaries (HAGBs) were defined as having misorientation differences between adjacent points higher than 15º and low-angle grain boundaries (LAGBs) had misorientations within the range from 2 to 15º.

3. Experimental results

Figure 1 shows the variation of the Vickers microhardness along the diameter of the Al-3Mg-0.2Sc discs processed through 10 turns of HPT at 450 K and further annealed at different temperatures. It is readily noted from these plots that there is a significant increase in the microhardness of the solution treated material after 10 turns of HPT at an elevated temperature. The Vickers microhardness of the unprocessed alloy is ~58 Hv whereas hardness values as high as ~185 Hv were detected in the HPT-processed sample as noted in the hardness measurements denoted by open circles. Furthermore, although higher hardness values were attained in the same alloy after HPT at 300 K [32], the metal processed by HPT at 450 K displays a more uniform microhardness distribution with hardness values varying from ~160 to ~185 Hv at the centre and near to the periphery of the disc, respectively.

It follows from Fig. 1 that post-HPT annealing at 473 K leads to a slight decrease in the hardness recorded along the diameter of the Al-3Mg-0.2Sc sample, but nevertheless the overall shape of the microhardness distribution remains unchanged. In addition, the microhardness distribution in the HPT-processed metal becomes reasonable homogeneous after annealing at $T > 473$ K, although the hardness values continue decreasing with increasing temperatures.

Figure 2 displays the variation of the area-weighted average microhardness with the annealing temperature for the Al-3Mg-0.2Sc alloy processed through 10 turns of HPT at room temperature [33] or at 450 K and further annealed for 1 h. The results demonstrate that the average microhardness of the material examined in this study is ~180 Hv after 10 turns of HPT at 450 K. Furthermore, there is a minor reduction in the average microhardness after annealing at $T \leq 473$ K wherein the Vickers microhardness is ~160 Hv. By contrast, it is clearly evident that annealing at temperatures within the interval from 523 to 623 K leads to a more significant decrease in the hardness values which continue to decline but at lower rates for $T \geq 673$ K.

It is also apparent from Fig. 2 that the Al-3Mg-0.2Sc alloy processed through 10 turns of HPT at 300 K exhibits higher hardness values immediately after processing compared with

the same alloy processed by HPT at 450 K. Nevertheless, it was consistently verified that after subsequent annealing at $T \geq 473$ K the material processed by HPT at an elevated temperature displayed superior microhardness as a consequence of the more rapid softening kinetics for the material deformed at room temperature.

The grain boundaries of the Al-3Mg-0.2Sc alloy were revealed after etching using a solution of 5 % HBF_4 dissolved in water. Afterwards, various SEM images were taken in this material at positions located at distances of ~3 mm from the centres of the discs in order to estimate the average grain size after HPT at 450 K and subsequent annealing at different temperatures, as depicted in Fig. 3. For comparison purposes, additional datum points are included for the same material processed by HPT at ambient temperature and further annealed at equivalent conditions [33].

Figure 3 reveals that the grain size of the Al alloy processed through 10 turns of HPT at 450 K is ~0.15 μm. There is only a limited grain coarsening after heat treatment at $T \leq 523$ K, as $d < 0.23$ μm even after annealing for 1 h. Conversely, significant grain growth occurs during annealing at temperatures ranging from 573 to 673 K in which the grain sizes after annealing are ~0.35 and 1.48 μm, respectively. Furthermore, it is apparent that the coarsening rate decreases to almost negligible values for $T > 673$ K such that $d < 2$ μm after annealing at 773 K for 1 h.

It is interesting to note that the average grain size in the Al-3Mg-0.2Sc alloy subjected to HPT at ambient temperature was only slightly inferior to the values measured in the same metal immediately after HPT at 450 K. However, the experimental data displayed in Fig. 3 demonstrate that the grain structures developed in the Al alloy during HPT processing at 300 K are less stable and significant grain coarsening was noted after annealing at $T > 423$ K.

Figure 4 shows typical OIM images of the Al-3Mg-0.2Sc alloy after HPT processing at 450 K and subsequent annealing for 1 h at (a) 573, (b) 623 and (c) 773 K. The grains in these

images were coloured using a rainbow spectrum such that small grains are blue and large structures with HAGBs are filled with shades of red. It is clearly demonstrated in Fig. 4 (a) that the HPT-processed metal has a fairly homogeneous distribution of UFG structures after annealing at 573 K for 1 h. In addition, most of these structures are formed by HAGBs as subgrains are rarely visible in the OIM image.

By contrast, it is readily apparent from Fig. 4 (b) that there is the onset of a bi-modal distribution of grains in the Al-Mg-Sc alloy annealed at 623 K for 1 h. The ultrafine grains coloured in shades of blue are uniformly distributed and represent more than 70 % of the area fraction of the examined microstructure. A more detailed inspection of Fig. 4 (b) revealed the grain structures were essentially equiaxed and substructures developed within some of the larger grains during annealing at 623 K. In addition, the average grain size and the amount of LAGBs in the Al alloy further increased after heat treatment at 773 K for 1 h as observed in Fig. 4 (c).

4. Discussion

This investigation reveals that processing through 10 turns of HPT at 450 K leads to a lower average microhardness (~180 Hv) and slightly larger grain sizes (~0.15 μm) in the Al-3Mg-0.2Sc alloy compared with HPT at room temperature [33]. These results are consistent with earlier studies that examined the effect of the processing temperature on the restoration mechanisms during high-pressure torsion [26,34]. Accordingly, lower hardness values and larger grain sizes are attained after HPT processing at increasing homologous temperatures and this is attributed to a more significant contribution of dynamic softening mechanisms such as recovery and recrystallization during severe plastic deformation, as observed in pure nickel [26], palladium and copper [34].

The plots depicted in Fig. 3 and 4 consistently confirm that the microstructural stability of Al-Mg-Sc alloys processed by HPT is notably improved by conducting this procedure at an elevated temperature. The Al-3Mg-0.2Sc alloy subjected to 10 turns of HPT at 300 K and

annealed at 623 K exhibits an inhomogeneous microstructure formed by the few remaining fine grains and a large fraction of coarse grain structure with an average size of >10 μm [33] which is similar to the duplex structures reported for pure nickel processed by HPT at 300 K and further annealed at 448 K for 1 h [26]. By contrast, the Al alloy processed by HPT at 450 K displays a more uniform distribution of grains after annealing at 623 K. Although, there are a few grains with an average size of >2 μm, these HAGBs structures represent less than 10 % of the total amount of grains observed in Fig. 4 (b).

The temperature rise of the Al-3Mg-0.2Sc alloy after 10 turns of HPT processing at ambient temperature was calculated as ~30 K using an empirical relationship [35,36]. By considering this increase in the temperature of the sample, a maximum homologous temperature, T/T_m, of ~0.34 was estimated for the material processed at room temperature whereas T/T_m is ~0.51 during HPT processing at 450 K.

Dynamic recovery becomes more important and the rate of annihilation of dislocations increases during plastic straining at higher homologous temperatures. Accordingly, the strain energy stored in the form of microstructural defects is diminished in Al-Mg-Sc alloys processed by HPT at elevated temperatures as indicated by differential scanning calorimetry analysis conducted on an Al-5Mg-0.3Sc-0.08Zr alloy processed by HPT at different temperatures [37]. Therefore, as the strain energy provides the driving force for recrystallization, higher annealing temperatures are needed to start this phenomenon in the Al-3Mg-0.2Sc alloy processed by HPT at 450 K by comparison with the alloy processed at ambient temperature.

The grain boundary strengthening during plastic straining at low homologous temperatures may be expressed in terms of the Hall-Petch relationship considering the Vickers microhardness, H, and the average grain size, *d*, as follows [38]:

$$H = H_0 + k_H d^{-1/2} \quad (1)$$

where H_0 and k_H are material constants.

There are numerous studies discussing the validity of the Hall-Petch relationship for different Al-Mg-Sc alloys after SPD processing [18,33,39,40]. In order to examine the range of grain sizes in which this relationship remains accurate and assess the effect of the Mg content on the mechanical properties of Al-Mg-Sc alloys, the Vickers microhardness was plotted as a function of $d^{-1/2}$ for the Al-3Mg-0.2Sc alloy processed by HPT at 450 K as well as for similar Al-Mg-Sc alloys processed by HPT at ambient temperatures [33,37] or ECAP [17,18,20,41], as depicted in Fig. 5.

It is readily apparent from Fig. 5 that there is a linear relationship between H and $d^{-1/2}$ for the Al-3Mg-0.2Sc alloy processed by HPT at an elevated temperature. Furthermore, all the experimental datum points referring to Al-Mg-Sc alloys with ~3 % Mg in weight lie close to a single line with H_0 = 28.7 Hv and $k_H \approx 0.056$ Hv $m^{-1/2}$.

For comparison purposes, additional data was included for an Al-Mg-Sc-Zr alloy with higher Mg contents [18,20,41]. This Al alloy was subjected to ECAP at elevated temperatures such that grain sizes as high as ~1 μm were obtained after ECAP [18]. It is clearly noted in Fig. 5 that the Al-Mg-Sc-Zr alloys with 5 and 6 % of Mg display increased hardness values by comparison with the Al-3Mg-0.2Sc alloy having the same average grain sizes. This additional hardening is a direct consequence of solid solution strengthening caused by the addition of Mg in solid solution. Nevertheless, the Hall-Petch relationship remains accurate for the ECAP-processed material with $d^{-1/2} < 1000$ $m^{-1/2}$ and $k_H \approx 0.056$ Hv $m^{-1/2}$ for Al-Mg-Sc alloys with higher Mg contents.

Figure 5 also reveals an apparent breakdown in the Hall-Petch relationship in Al-Mg-Sc alloys with d < ~50 nm. This is consistent with a study wherein the grain boundary strengthening was accurately predicted using this relationship for Al-Mg-Sc alloys having grain sizes down to ~94 nm [40]. By contrast, grain refinement provides no further increase in the

yield strength in pure aluminium and Al-Mg alloys without Sc additions for grain sizes smaller than ~400 and ~150 nm, respectively.

The breakdown in the Hall-Petch relationship in nanostructured metals is usually attributed to the action of different deformation mechanisms such as dislocation emission at grain boundaries and the increasing contribution of grain boundary sliding [42]. Accordingly, the extended validity of the Hall-Petch relationship in Al-Mg-Sc alloys is associated with the segregation of Mg at grain boundaries and triple junctions during SPD processing [39,40]. In practice, these segregations reduce the boundary energy and ultimately increase the local stress needed for the emission of extrinsic dislocations [43].

Nevertheless, it is interesting to note that Mg segregation is observed in the Al-5.7Mg-0.32Sc alloy processed by HPT [44] at similar conditions as in the experimental datum points displaying no further increase in the hardness values with decreasing grain sizes. Therefore, a more comprehensive study is needed to determine whether the breakdown occurs because grain boundary sliding becomes active at low deformation temperatures or the applied stress is sufficiently high to promote the emission and annihilation of dislocations at grain boundaries in the Al-Mg-Sc alloy with average grain sizes <50 nm.

Severe plastic deformation through HPT processing at room temperature promotes further strain hardening and grain refinement in Al-Mg-Sc alloys [32,37,39,45-47] by comparison with ECAP [17,18-20,40,48]. Conversely, the elongations to failure after tensile testing at superplastic conditions are notable inferior [45-47,49] as a consequence of the advent of abnormal grain growth at $T \geq 623$ K [33]. Although, the onset of a bi-modal distribution of grains is also observed in the Al-3Mg-0.2Sc alloy processed through 10 turns of HPT at 450 K, the grains structures in this alloy are mostly formed by HAGBs and remain essentially ultrafine ($d \approx 0.85$ μm) even after annealing at 623 K. It is concluded therefore that the microstructural stability in Al-Mg-Sc alloys is significantly improved by

conducting HPT processing at 450 K and this permits the retention of the benefits obtained through grain refinement and the ability to achieve superior superplastic properties at high temperatures.

5. Summary and conclusions

1. An Al-3% Mg-0.2% Sc alloy was processed through 10 turns of HPT at 450 K to produce a grain size of ~150 nm. Thereafter, annealing was conducted for 1 h at temperatures from 423 to 773 K.

2. A reasonably uniform hardness distribution with an average microhardness of ~180 Hv was obtained in the Al alloy after HPT. There was a continuous reduction in the hardness values during annealing at increasing temperatures, especially for $T \geq 523$ K.

3. The microstructural stability in Al-Mg-Sc alloys was significantly improved by conducting HPT at 450 K. Dynamic recovery became more significant during HPT at high homologous temperatures and reduced the strain energy stored in the Al alloy.

4. The microstructure is more homogeneous and the grain coarsening kinetics are delayed in the UFG metal processed by HPT at 450 K by comparison with the same alloy processed by HPT at 300 K. The grain structures were mostly formed by HAGBs and the average grain sizes were <2 μm after annealing for 1 h at 773 K.

Acknowledgements

This work was supported by CAPES in Brazil and by the European Research Council under ERC Grant Agreement No. 267464-SPDMETALS.

References

[1] Miller WS, Zhuang L, Bottema J, Wittebrood AJ, De Smet P, Haszler A, Vieregge A. Recent development in aluminium alloys for the automotive industry. Mater Sci Eng A 2000;280:37-49.

[2] Valiev RZ, Islamgaliev RK, Alexandrov IV. Bulk nanostructured materials from severe plastic deformation. Prog Mater Sci 2000;45:103-89.

[3] Langdon TG. Twenty-five years of ultrafine-grained materials: Achieving exceptional properties through grain refinement. Acta Mater 2013;61:7035-59.

[4] Sabirov I, Murashkin MYu, Valiev RZ. Nanostructured aluminium alloys produced by severe plastic deformation: New horizons in development. Mater Sci Eng A 2013;560:1-24.

[5] Valiev RZ, Langdon TG. Principles of equal-channel angular pressing as a processing tool for grain refinement. Prog Mater Sci 2006;51:881-981.

[6] Zhilyaev AP, Langdon TG. Using high-pressure torsion for metal processing: Fundamentals and applications. Prog Mater Sci 2008;53:893-979.

[7] Figueiredo RB, Cetlin PR, Langdon TG. The processing of difficult-to-work alloys by ECAP with an emphasis on magnesium alloys. Acta Mater 2007;55:4769-79.

[8] Iwahashi Y, Horita Z, Nemoto M, Langdon TG. Factors influencing the equilibrium grain size in equal-channel angular pressing: Role of Mg additions to aluminum. Metall Mater Trans A 1998;29:2503-10.

[9] Gubicza J, Chinh NQ, Horita Z, Langdon TG. Effect of Mg addition on microstructure and mechanical properties of aluminium. Mater Sci Eng A 2004;387-389:55-9.

[10] Chen YJ, Chai YC, Roven HJ, Gireesh SS, Yu YD, Hjelen J. Microstructure and mechanical properties of Al-xMg alloys processed by room temperature ECAP. Mater Sci Eng A 2012;545:139-47.

[11] Andreau O, Gubicza J, Zhang NX, Huang Y, Jenei P, Langdon TG. Effect of short-term annealing on the microstructures and flow properties of an Al-1% Mg alloy processed by high-pressure torsion. Mater Sci Eng A 2014;615:231-9.

[12] Lee HJ, Han JK, Janakiraman S, Ahn B, Kawasaki M, Langdon TG. Significance of grain refinement on microstructure and mechanical properties of an Al-3% Mg alloy processed by high-pressure torsion. J Alloys Compd 2016;686:998-1007.

[13] Wang J, Iwahashi Y, Horita Z, Furukawa M, Nemoto M, Valiev RZ, et al. An investigation of microstructural stability in an Al-Mg alloy with submicrometer grain size. Acta Mater 1996;44:2973-82.

[14] Morris DG, Muñoz-Morris MA. Microstructure of severely deformed Al-3Mg and its evolution during annealing. Acta Mater 2002;50:4047-60.

[15] Lee S, Utsunomiya A, Akamatsu H, Neishi K, Furukawa M, Horita Z, et al. Influence of scandium and zirconium on grain stability and superplastic ductilities in ultrafine-grained Al–Mg alloys. Acta Mater 2002;50:553-64.

[16] Røyset J, Ryum N. Scandium in aluminium alloys. Int Mater Rev 2005;50:19-44.

[17] Dám K, Lejček P, Michalcová A. In situ TEM investigation of microstructural behavior of superplastic Al-Mg-Sc alloy. Mater Charact 2013;76:69-75.

[18] Avtokratova E, Sitdikov O, Mukhametdinova O, Markushev M, Narayana Murty SVS, Prasad MJNV,et al. Microstructural evolution in Al-Mg-Sc-Zr alloy during severe plastic deformation and annealing. J Alloys Compd 2016;673:182-94.

[19] Komura S, Horita Z, Furukawa M, Nemoto M, Langdon TG. An evaluation of the flow behavior during high strain rate superplasticity in an Al-Mg-Sc alloy. Metall Mater Trans A 2001;32:707-16.

[20] Sitdikov O, Sakai T, Avtokratova E, Kaibyshev R, Kimura Y, Tsuzaki K. Grain refinement in a commercial Al-Mg-Sc alloy under hot ECAP conditions. Mater Sci Eng A 2007;444:18-30.

[21] Avtokratova E, Sitdikov O, Markushev M, Mulyukov R. Extraordinary high-strain rate superplasticity of severely deformed Al-Mg-Sc-Zr alloy. Mater Sci Eng A 2012;538:386-90.

[22] Harai Y, Kai M, Kaneko K, Horita Z, Langdon TG. Microstructural and mechanical characteristics of AZ61 magnesium alloy processed by high-pressure torsion. Mater Trans 2008;49:76-83.

[23] Kai M, Horita Z, Langdon TG. Developing grain refinement and superplasticity in a magnesium alloy processed by high-pressure torsion. Mater Sci Eng A 2008;488:117-24.

[24] Abramova MM, Enikeev NA, Sauvage X, Etienne A, Radiguet B, Ubyivovk E, et al. Thermal stability and extra-strength of an ultrafine grained stainless steel produced by high pressure torsion. Rev Adv Mater Sci 2015;43:83-8.

[25] Dobatkin SV, Rybalchenko OV, Enikeev NA, Tokar AA, Abramova MM. Formation of fully austenitic ultrafine-grained high strength state in metastable Cr–Ni–Ti stainless steel by severe plastic deformation. Mater Lett 2016;166:276-9.

[26] Ghosh P, Renk O, Pippan R. Microtexture analysis of restoration mechanisms during high pressure torsion of pure nickel. Mater Sci Eng A 2017;684:101-9.

[27] Figueiredo RB, Cetlin PR, Langdon TG. Using finite element modeling to examine the flow processes in quasi-constrained high-pressure torsion. Mater Sci Eng A 2011;528:8198-204.

[28] Pereira PHR, Figueiredo RB, Cetlin PR, Langdon TG. Using finite element modeling to examine the flow process and temperature evolution in HPT under different constraining conditions. IOP Conference Series: Materials Science and Engineering. 2014;63:012041.

[29] Figueiredo R, Langdon TG. Development of structural heterogeneities in a magnesium alloy processed by high-pressure torsion. Mater Sci Eng A 2011;528:4500-6.

[30] Pereira PHR, Figueiredo RB, Cetlin PR, Langdon TG. An examination of the elastic distortions of anvils in high-pressure torsion. Mater Sci Eng A 2015;631:201-8.

[31] Kawasaki M, Langdon TG. The significance of strain reversals during processing by high-pressure torsion. Mater Sci Eng A 2008;498:341-48.

[32] Pereira PHR, Huang Y, Langdon TG. Influence of initial heat treatment on the microhardness evolution of an Al-Mg-Sc alloy processed by high-pressure torsion. Mater Sci Forum 2017;879:1471-6.

[33] Pereira PHR, Huang Y, Langdon TG. Examining the thermal stability of an Al-Mg-Sc alloy processed by high-pressure torsion. Mat Res 2017; submitted for publication.

[34] Edalati K, Horita Z. Significance of homologous temperature in softening behavior and grain size of pure metals processed by high-pressure torsion. Mater Sci Eng A 2011;528:7514-23.

[35] Figueiredo RB, Pereira PHR, Aguilar MTP, Cetlin PR, Langdon TG. Using finite element modeling to examine the temperature distribution in quasi-constrained high-pressure torsion. Acta Mater 2012;60:3190-8.

[36] Pereira PHR, Figueiredo RB, Huang Y, Cetlin PR, Langdon TG. Modeling the temperature rise in high-pressure torsion. Mater Sci Eng A 2014;593:185-8.

[37] Dobatkin SV, Zakharov VV, Vinogradov AYu, Kitagawa K, Krasil'nikov NA, Rostova TD, et al. Nanocrystalline structure formation in Al–Mg–Sc Alloys during severe plastic deformation. Russ Metall (Metally). 2006;6:533-40.

[38] Furukawa M, Horita Z, Nemoto M, Valiev RZ, Langdon TG. Microhardness measurements and the Hall-Petch relationship in an Al-Mg alloy with submicrometre grain size. Acta Mater 1996;44:4619-29.

[39] Valiev RZ, Enikeev NA, Murashkin MY, Kazykhanov VU, Sauvage X. On the origin of the extremely high strength of ultrafine-grained Al alloys produced by severe plastic deformation. Scr Mater 2010;63:949-52.

[40] Pereira PHR, Wang YC, Huang Y, Langdon TG. Influence of grain size on the flow properties of an Al-Mg-Sc alloy over seven orders of magnitude of strain rate. Mater Sci Eng A 2017;685:367-76.

[41] Sitdikov O, Avtokratova E, Sakai T, Tsuzaki K. Ultrafine-grain structure formation in an Al-Mg-Sc alloy during warm ECAP. Metall Mater Trans A 2013;44:1087-100.

[42] Meyers MA, Mishra A, Benson DJ. Mechanical properties of nanocrystalline materials. Prog Mater Sci 2006;51:427-556.

[43] Abdeljawad F, Foiles SM. Stabilization of nanocrystalline alloys via grain boundary segregation: a diffuse interface model. Acta Mater 2015;101:159-71.

[44] Sauvage X, Enikeev N, Valiev R, Nasedkina Y, Murashkin M. Atomic-scale analysis of the segregation and precipitation mechanisms in a severely deformed Al-Mg alloy. Acta Mater 2014;72:125-36.

[45] Sakai G, Horita Z, Langdon TG. Grain refinement and superplasticity in an aluminum alloy processed by high-pressure torsion. Mater Sci Eng A 2005;393:344-51.

[46] Perevezentsev VN, Shcherban MY, Murashkin MY, Valiev RZ. High-strain-rate superplasticity of nanocrystalline aluminum alloy. Tech Phys Lett 2007;33:648-50.

[47] Horita Z, Langdon TG. Achieving exceptional superplasticity in a bulk aluminum alloy processed by high-pressure torsion. Scr Mater 2008;58:1029-32.

[48] Zhemchuzhnikova D, Kaibyshev R. Mechanical behavior of an Al-Mg-Mn-Sc alloy with an ultrafine grain structure at cryogenic temperatures. Adv Eng Mater 2015;17:1804-11

[49] Pereira PHR, Huang Y, Langdon TG. Examining the mechanical properties and superplastic behaviour in an Al-Mg-Sc alloy after processing by HPT. Lett Mater 2015;5:294-300.

Figure captions:

Fig. 1. Variation of the average microhardness recorded at the middle-section position with distance from the centre of the Al-3Mg-0.2Sc discs after processing by HPT at 450 K and subsequent annealing.

Fig. 2. Average microhardness as a function of annealing temperature for the Al-3Mg-0.2Sc alloy processed by 10 turns of HPT at 450 K and annealed for 1 h at different temperatures: for comparison purposes, additional datum points are included for the Al-3Mg-0.2Sc alloy processed by HPT at 300 K and further annealed at identical conditions [33].

Fig. 3. Grain size as a function of annealing temperature for the Al-3Mg-0.2Sc alloy processed by 10 turns of HPT at 450 K and further annealed for 1 h at temperatures from 423 to 773 K: for comparison purposes, additional datum points are included for the Al-3Mg-0.2Sc alloy processed by HPT at 300 K and further annealed at identical conditions [33].

Fig. 4. Grain size coloured images of the grain structures of the Al-3Mg-0.2Sc alloy processed by 10 turns of HPT at 450 K and further annealed for 1 h at (a) 573, (b) 623 and (c) 773 K.

Fig. 5. Plot of Vickers microhardness as a function of $d^{-1/2}$ for the Al-3Mg-0.2Sc alloy processed by HPT at 450 K and subsequent annealing: Additional datum points are included for similar Al-Mg-Sc alloys processed by HPT [33,37] or ECAP [17,18,20,41].

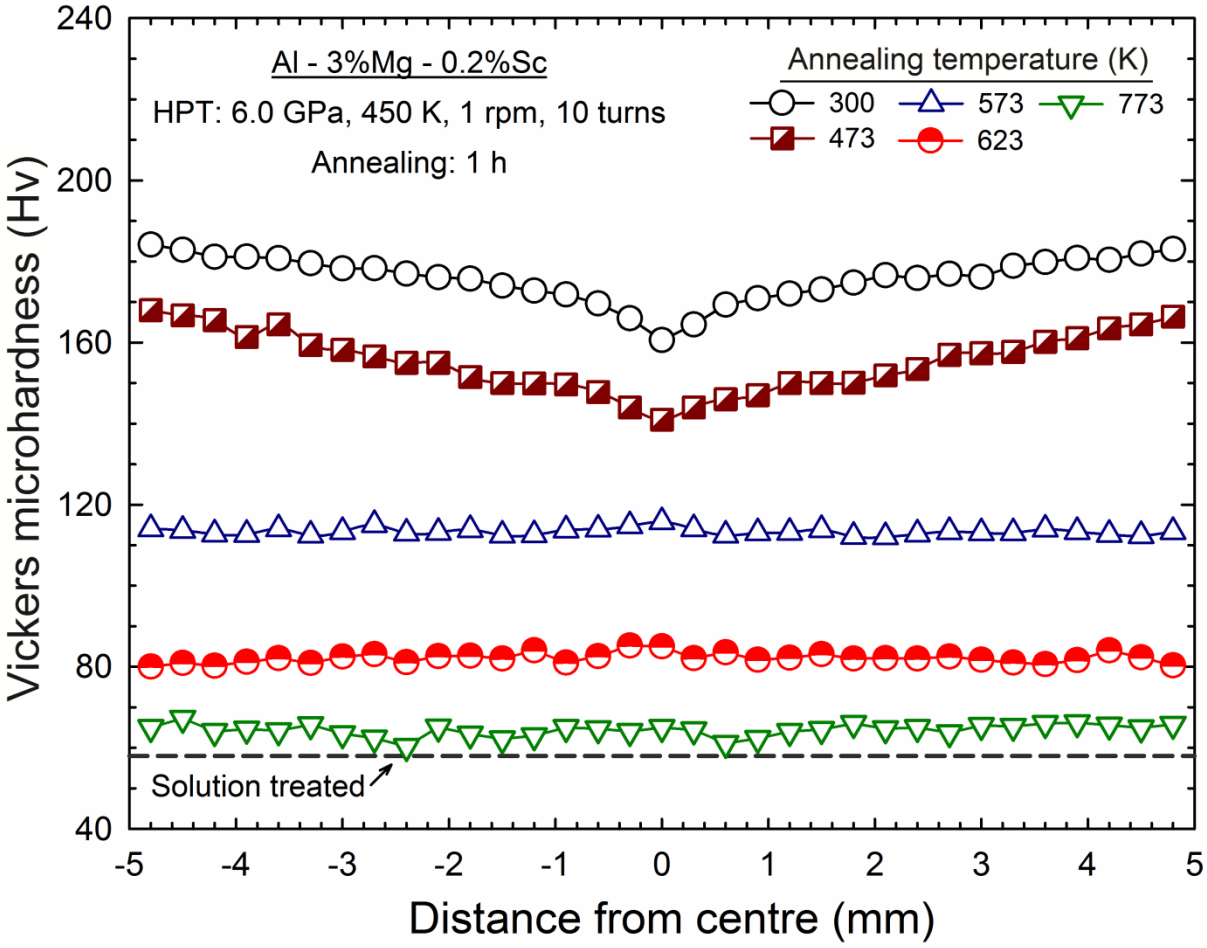
Al - 3%Mg - 0.2%Sc
HPT: 6.0 GPa, 450 K, 1 rpm, 10 turns
Annealing: 1 h
Annealing temperature (K)
300
573
773
473
623
Solution treated
Vickers microhardness (Hv)
Distance from centre (mm)
240
200
160
120
80
40
-5
-4
-3
-2
-1
0
1
2
3
4
5

Fig. 1

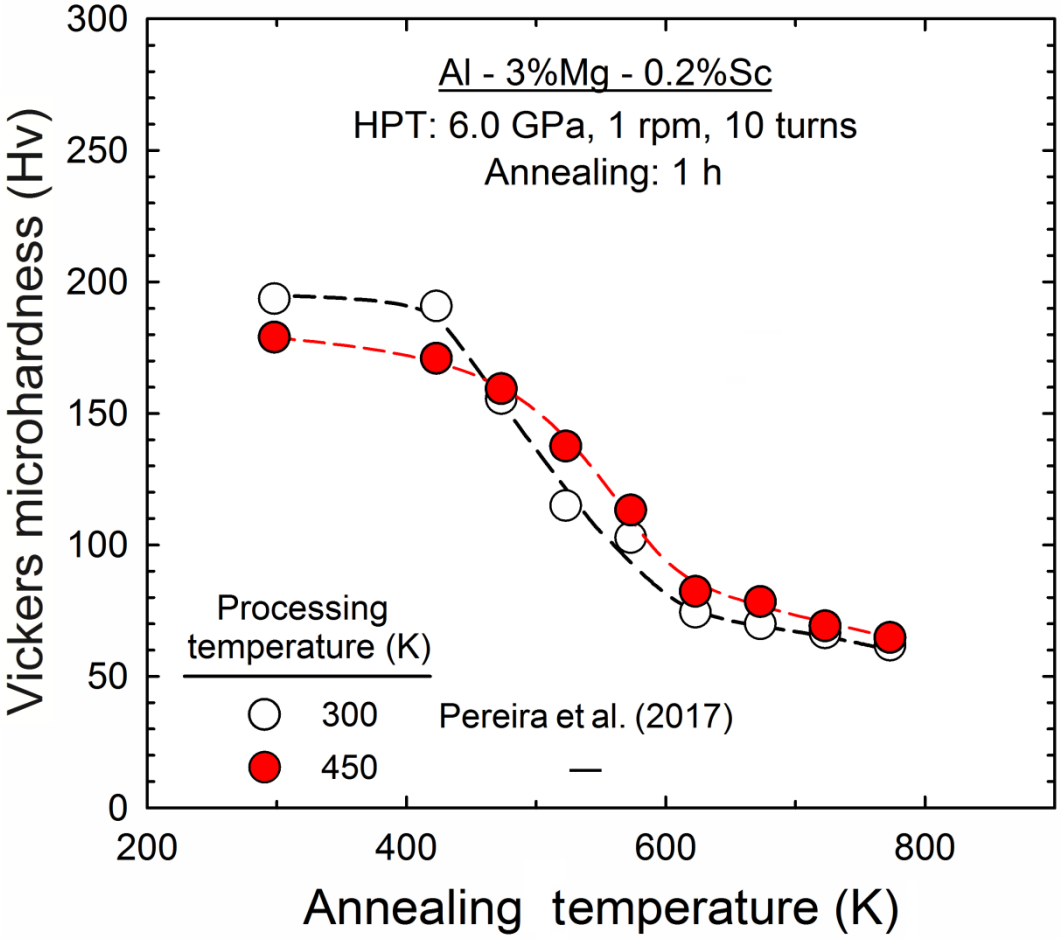
Al - 3%Mg - 0.2%Sc
HPT: 6.0 GPa, 1 rpm, 10 turns
Annealing: 1 h
Processing temperature (K)
300
450
Pereira et al. (2017)
Vickers microhardness (Hv)
Annealing temperature (K)
0
50
100
150
200
250
300
200
400
600
800

Fig. 2

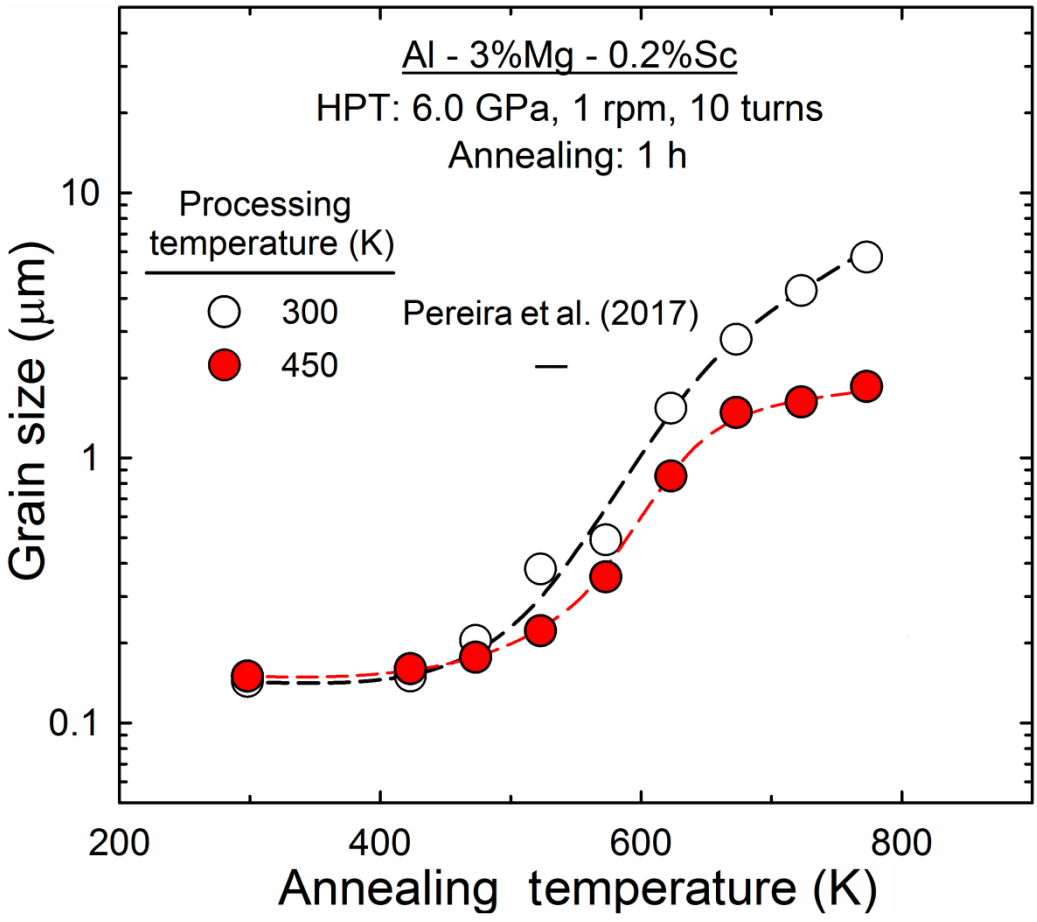
Al - 3%Mg - 0.2%Sc
HPT: 6.0 GPa, 1 rpm, 10 turns
Annealing: 1 h
Processing temperature (K)
300
450
Pereira et al. (2017)
Grain size (μm)
10
1
0.1
200
400
600
800
Annealing temperature (K)

Fig. 3

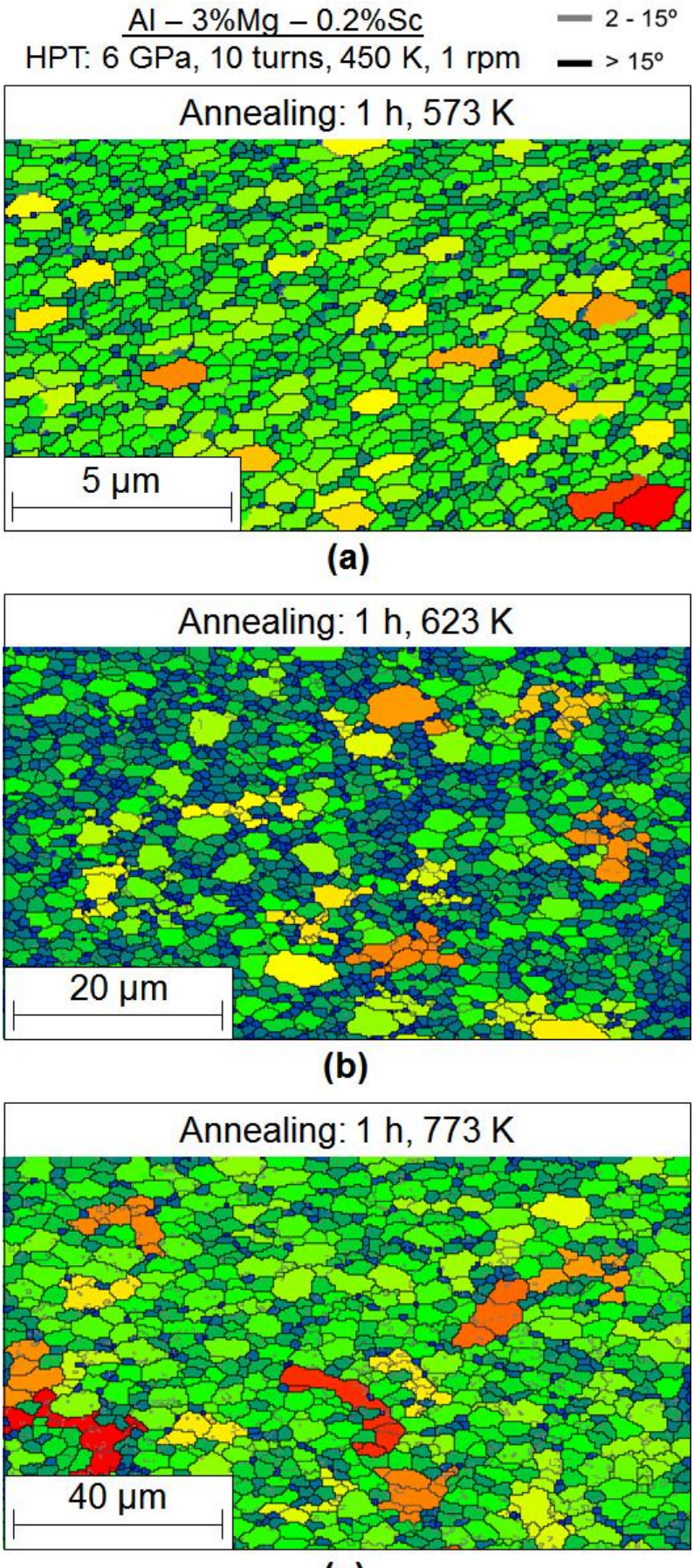
Al – 3%Mg – 0.2%Sc
HPT: 6 GPa, 10 turns, 450 K, 1 rpm
2 - 15°
> 15°
Annealing: 1 h, 573 K
5 μm
(a)
Annealing: 1 h, 623 K
20 μm
(b)
Annealing: 1 h, 773 K
40 μm
(c)

Fig. 4

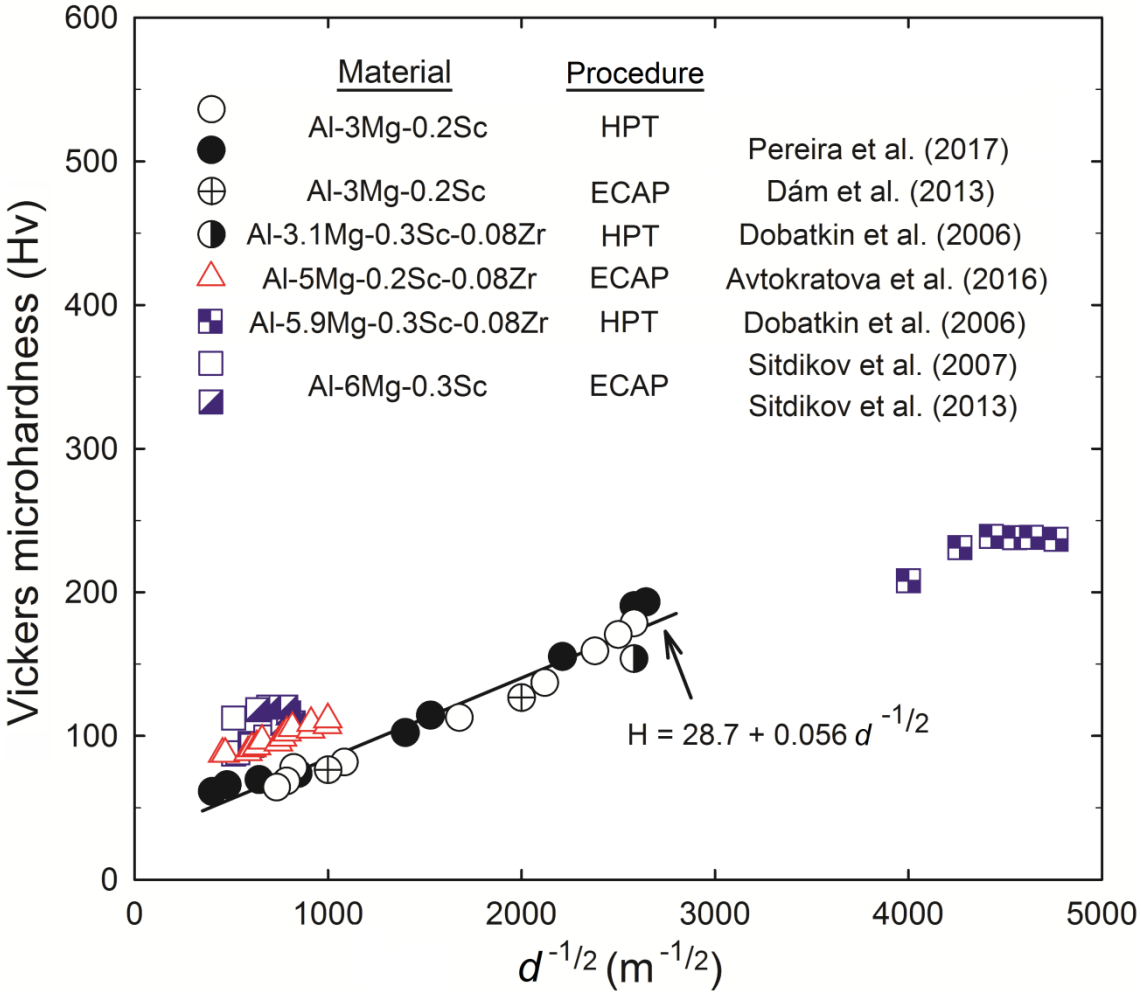
Material
Procedure
Al-3Mg-0.2Sc
HPT
Pereira et al. (2017)
Al-3Mg-0.2Sc
ECAP
Dám et al. (2013)
Al-3.1Mg-0.3Sc-0.08Zr
HPT
Dobatkin et al. (2006)
Al-5Mg-0.2Sc-0.08Zr
ECAP
Avtokratova et al. (2016)
Al-5.9Mg-0.3Sc-0.08Zr
HPT
Dobatkin et al. (2006)
Al-6Mg-0.3Sc
ECAP
Sitdikov et al. (2007)
Sitdikov et al. (2013)
H = 28.7 + 0.056 d -1/2
Vickers microhardness (Hv)
d -1/2 (m -1/2)
0
100
200
300
400
500
600
0
1000
2000
3000
4000
5000

Fig. 5